Talanta 298 (2026) 129004

Contents lists available at ScienceDirect

Talanta

journal homepage: www.elsevier.com/locate/talanta

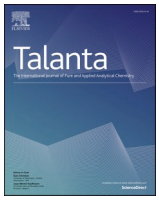

Hollow fiber flow field-flow fractionation enables high-quality Extracellular Vesicle isolation from minimal plasma samples in polycythemia vera liquid biopsy

Ghazal Narimanfar [a,1], Anna Placci [b,c,d,1], Filippo Maltoni [e], Stefano Giordani [b,c,d], Gianluca Storci [f], Barbara Roda [b,c,d], Andrea Zattoni [b,c,d], Pierluigi Reschiglian [b,c,d], Massimiliano Bonafè [a,f], Francesca Palandri [e], Valentina Marassi [b,c,d,*], Lucia Catani [a,e,**]

[a] Department of Medical and Surgical Sciences, University of Bologna, Bologna, Italy
[b] Department of Chemistry "G. Ciamician", University of Bologna, Bologna, Italy
[c] byFlow srl, Bologna, Italy
[d] Biostructures and Biosystems National Institute (INBB), Rome, Italy
[e] IRCCS Azienda Ospedaliero-Universitaria di Bologna, Istituto di Ematologia "Seràgnoli", Bologna, Italy
[f] IRCCS Azienda Ospedaliero-Universitaria di Bologna, Bologna, Italy

ARTICLE INFO

Handling editor: Qun Fang

Keywords:
Extracellular vesicles
Hollow-fiber flow field-flow fractionation
Size exclusion chromatography
Polycythemia vera
Liquid biopsy

ABSTRACT

Introduction: Extracellular vesicles (EVs) are crucial mediators of intercellular communication, transporting various macromolecules between cells. They are increasingly recognized for their roles in cancer progression, immune modulation, and therapeutic resistance. However, standard EV isolation methods often struggle to preserve EV heterogeneity and functional integrity.

Methods: In this study, we used hollow-fiber flow field-flow fractionation (HF5) to isolate and characterize plasma-derived EVs from just 60 μL of plasma. HF5 is a cutting-edge, disposable microfluidic technique designed for advanced EV fractionation. EVs were from patients with polycythemia vera (PV), a rare hematological malignancy. We evaluated EVs isolated using HF5 against those obtained by size-exclusion chromatography (SEC), assessing their physico-chemical characteristics, surface marker expression and functionality in terms of up taking and inflammatory potential.

Results: EVs isolated through HF5 closely resembled SEC-derived EVs in size, morphology, and classical EV markers, including platelet-specific proteins. HF5 consistently yielded purer EV preparations with reduced aggregation and greater reproducibility. Notably, HF5 achieved this using 8.3 times less plasma than SEC. HF5 EVs, along with inflammatory potential, showed superior cell up take to the SEC counterparts. Chemical analysis showed that HF5-EVs contained a higher protein concentration, while SEC-EVs had more aggregated material.

Conclusion: HF5 integrates EV isolation and characterization, enhancing efficiency, and preserving sample integrity and functionality. Its minimal sample requirement and reproducibility make it particularly suitable for clinical and translational research. Our study demonstrated HF5 as a powerful better alternative to conventional EV isolation methods, with strong potential for standardized applications in biomarker discovery and cancer research.

* Corresponding author. Department of Chemistry "G. Ciamician", University of Bologna, Bologna, Italy
** Corresponding author. IRCCS Azienda Ospedaliero-Universitaria di Bologna, Istituto di Ematologia "Seràgnoli", Bologna, Italy.
E-mail addresses: ghazal.narimanfar2@unibo.it (G. Narimanfar), anna.placci3@unibo.it (A. Placci), filippo.maltoni2@unibo.it (F. Maltoni), stefano.giordani7@unibo.it (S. Giordani), gianluca.storci@aosp.bo.it (G. Storci), barbara.roda@unibo.it (B. Roda), andrea.zattoni@unibo.it (A. Zattoni), pierluigi.reschiglian@unibo.it (P. Reschiglian), massimiliano.bonafe@unibo.it (M. Bonafè), francesca.palandri@unibo.it (F. Palandri), valentina.marassi@unibo.it (V. Marassi), lucia.catani@unibo.it (L. Catani).
[1] Contributed equally.

https://doi.org/10.1016/j.talanta.2025.129004
Received 28 July 2025; Received in revised form 14 October 2025; Accepted 16 October 2025
Available online 17 October 2025

1. Introduction

Extracellular vesicles (EVs), which are lipid-bilayer-enclosed particles released from all cell types, facilitate intercellular communication by transferring bioactive macromolecules such as nucleic acids, proteins, metabolites, and lipids between cells [1–3]. Peripheral blood contains EVs derived from platelets/megakaryocytes, red blood cells, leukocytes, and endothelial cells; however, platelet/megakaryocyte-derived EVs are the most abundant. Based on size and biogenesis, Small (*S*-; 30–200 nm) and Large (L-; 0.2–10 μm) EVs can be identified [4–6]. EVs are critical players in the regulation of immunity and inflammation that, in turn, may contribute to the further release of EVs. Importantly, due to their diagnostic and prognostic potential, EV-based liquid biopsy is gaining growing attention in the tumor microenvironment (TME) [7].

However, the isolation of EVs from biological fluids, including blood, remains challenging. In fact, the high protein and lipid concentration in plasma presents a significant challenge in isolating a selected population of EVs. Various EV isolation techniques, including size-exclusion chromatography (SEC), ultracentrifugation, precipitation, and immunoaffinity isolation, have been developed, each offering distinct advantages but also presenting limitations like EV damage and aggregation. While these methods have significantly advanced EV research, they highlight the ongoing need for more specific, efficient, and minimally disruptive isolation techniques. Such approaches would enable the characterization of EVs under native conditions, thereby preserving the bioactivity of the biological macromolecules they carry and supporting their potential use in diagnostic and therapeutic applications [8–10].

Hollow-fiber flow field-flow fractionation (HF5) advances beyond the performance of common isolation techniques to enter the isolation pipeline of EV and biomaterials. Designed for efficient integration into analytical platforms, this microfluidic technology offers enhanced performance as an advanced fractionation technique [11,12]. HF5 is a miniaturized variation of asymmetric flow field-flow fractionation (AF4). As demonstrated by Oeyen et al., AF4 coupled with UV and multi-angle light scattering detectors (AF4/UV-MALS) represents an advanced method for EV isolation and characterization [13]. HF5 improves the fractionation approach by utilizing a small-volume tubular porous membrane. This significantly reduces sample dilution and increases separation efficiency [14]. Separation occurs under gentle conditions, preserving biological integrity [15–17]. Specifically, unlike other commonly used EV isolation approaches, HF5 operates under fully laminar and low-flow conditions that minimize hydrodynamic stress and prevent shear-induced alterations. Separation occurs exclusively by hydrodynamic size, without significant interactions between the analytes and the membrane surface. Although nonspecific adsorption can theoretically occur, such effects can be evaluated and monitored through Flow Injection Analysis (FIA) and Focus FIA (FFIA), which enable quantification of potential sample loss during the separation process [18,19]. Interestingly, HF5 can be utilized not only as an isolation tool but also to monitor the outcome of other separation techniques. This approach consists in the reinjection of an aliquot of isolated EVs with the same method accessing multidetector profiling in the same experimental conditions, allowing a direct comparison between different techniques, and immediate feedback on EV quality.

In a previous study, we combined HF5 with ultracentrifugation to isolate EVs from culture medium, providing comprehensive information on the sample composition, including DNA- and protein-containing particles, free DNA, and potential exomes. These findings demonstrated the ability of HF5 to effectively discriminate bioparticles based on their size and analyze their macromolecular composition [11]. The effective integration of this approach for biomarker quantification and cancer biology fingerprinting has, however, remained unseen to date, notwithstanding the huge interest in reducing sample amount in EV analysis from biological fluids, especially from blood samples, and the need for an effective and realistic unravelling of EV composition and content.

Polycythemia vera (PV) is a BCR::ABL-negative chronic Myeloproliferative neoplasm (MPN) characterized by the clonal expansion of the erythrocyte mass due to mutations in the Janus Kinase 2 (JAK2) gene that cause hyperactivation of JAK-STAT signalling [20]. PV patients suffer from a range of complications, including mild to severe thrombotic events, systemic symptoms, progressive splenomegaly, and progression to acute leukemia or secondary myelofibrosis [21–24]. Beyond molecular pathogenesis, PV is characterized by a state of chronic inflammation, which has been indicated as the main contributor in MPN initiation/clonal evolution [25–27]. However, despite the fact that EVs are having role to the inflammatory process, the role of EVs within PV -TME has been poorly investigated with most studies highlighting only the increased proportion of circulating EVs [28–30]. Only one study described the proteomic cargo of PV EVs showing that serum-derived EVs were enriched in platelet activation-, immune/inflammatory response-, coagulation- and angiogenesis-related biomarkers [31].

In this work we achieved isolation of EVs in their native state by employing HF5 as a first-line EV isolation method utilizing minimal amounts of plasma from patients with cancer such as PV. To demonstrate the validity of this new approach, we systematically compared the biological and chemical properties of EVs isolated using HF5 and with those obtained through SEC along with identification of selected biomarkers, achieving for the first time the biomarker fingerprint of PV in a single step of isolation and avoiding sample degradation.

2. Material and methods

2.1. Study cohort

This study includes PV patients at diagnosis (n = 10) and age-matched healthy donors (HDs, n = 6) followed at the Institute of Hematology "L. and A. Seràgnoli, IRCCS AOU S. Orsola-Malpighi, Bologna. Patients were diagnosed according to the 2022 WHO classification and carried the JAK2V617F mutation.

2.2. Blood sample collection and plasma preparation

Peripheral blood from PV patients and age/sex-matched HDs was collected in commercially available Vacutainer tubes containing ethylenediaminetetraacetic acid (EDTA) and serum tubes (BD Vacutainer, BD, USA). Blood samples were processed within 120 min after withdrawal. Platelet rich plasma (PRP) was obtained by centrifugation at 1000×*g* for 15 min at room temperature (RT). The PRP was then centrifuged at 2500×*g* for 15 min at RT. Platelet-poor plasma (PPP) was then aliquoted into protein low-binding tubes (Eppendorf, Germany) with 1% dimethylsulfoxide (DMSO) (Wak-Chemie Medical GmbH, Steinbach, Germany) and stored at −80 °C. Before EV isolation, PPP samples were defrosted at RT and centrifuged at 2500×*g* for 15 min at RT. In parallel, HD serum was obtained by centrifugation of whole blood at 1000×*g* for 15 min at RT.

2.3. HF5 optimization for the separation of EVs from human plasma

EVs were isolated from human plasma using the HF5 system, which integrates an Agilent 1200 HPLC system (Agilent Technologies, Santa Clara, CA, USA), including a degasser and an isocratic pump, with an Eclipse® DUALTEC separation module (Wyatt Technology Europe, Dernbach, Germany) to control HF5 flow rates and operations. The HF5 channel (Wyatt Technology Europe) was made up of a 17 cm-long polymeric hollow fiber sealed inside a plastic cartridge using two sets of ferrules, gaskets and cap nuts. The hollow fiber was made of a polyethersulfone (PES) fiber, of type FUS, with an internal diameter of 0.8 mm, an external diameter of 1.3 mm and a MW cut-off of 10 kDa, corresponding to an average pore diameter of 5 nm. The eluted species were

characterized using a series of online detectors, reported here in the order of coupling with the separative system: an Agilent 1100 DAD UV/Vis spectrophotometer, an 18-angle multiangle light scattering (MALS) detector DAWN HELEOS (Wyatt Technology Corporation, Santa Barbara, CA, USA) operating at a wavelength of 658 nm and an Agilent 1200 spectrofluorometer working using a 280 nm absorption wavelength and a 340 nm emission wavelength. The software ChemStation version B.04.02 (Agilent Technologies, Santa Clara, CA, USA) was used to control the instrumentation, set method parameters and for data collection. ASTRA® software version 6.1.7 (Wyatt Technology Corporation) was used to collect and handle MALS and UV signals in order to obtain molecular weight and size information for the analytes.

The HF5 method consists of four steps: focus, focus-injection, elution, and elution-injection. During the first two stages, the mobile phase converges from both inlet and outlet, and the sample is injected through the inlet and focused in a narrow band. In the elution only, the inlet flow is maintained and is split into a transversal component (cross-flow, Vx) which generates the separative field, while the remaining longitudinal flow (Vc) brings the analytes to the detectors. Lastly, elution-injection allows the injection line to be cleaned. The separation method was further developed starting from the study by Marassi et al. [18], where the feasibility of serum fractionation was shown, to minimize resolution within the molecular weight range of 30–200 kDa, characteristic of proteins, and to optimize the separation window for species with diameters exceeding 20 nm, and the parameters used for EV isolation are listed in Table 1. To simulate a physiological environment, isotonic PBS, pH 7.4, 0.22 μm filtered, was used as the mobile phase. Since plasma has a high viscosity, the samples (20 μL) were diluted in a 1:1 ratio in the mobile phase and a volume of 40 μL was injected.

Recovery was calculated as Focus FIA/FIA area ratio %, the two methods being a filtrating, non-separating injection and a non-filtrating, non-separating injection. The UV signal at 280 nm showed a recovery >95% for injections of standard bovine serum albumin (BSA) solutions (15 μl injections, n = 3) and >96% for plasma samples (2 μL of HD plasma was injected, n = 3 for recovery assessment).

Repeatability and reproducibility were assessed in retention times and signal intensity both intra- and inter-day (n = 3) for protein standard BSA. The deviations (15 μl injections) were less than 1% and 2% in terms of retention time and signal intensity, respectively. LOD (three-sigma) and LOQ (ten-sigma) for BSA were calculated to be 0.05 μg and 0.16 μg. The developed method followed the harmonized guideline ICHQ2R1 and ISO/TS 21362 criteria [32].

Each plasma sample was injected three times (total plasma injected: 60 μL) and a fraction was collected between 11 and 17 min, obtaining a 6.3 ml fraction. After optimization of cut-off, fractions were then concentrated using MWCO 100 kDa Amicon Ultra-2 Centrifugal (Millipore, Merck, USA) filter following the manufacturer's protocol. All samples were added DMSO (1%) and then stored at −80 °C until further use.

EVs derived from SEC and HF5 were also analyzed using HF5 multi-detection as a quality control and a direct comparison of the enriched content. We applied the same HF5 method (see Table 1), but this time with a 6-min-long elution-injection step to avoid carrying over. Concentrated fractions were diluted in a ratio of 1:10 in PBS, and an injection volume of 20 μL was set for SEC-derived EVs, while for HF5 fractions a volume of 25 μL was chosen.

Quantitative comparison of the species in SEC- and HF5-derived fractions was performed by integrating the peak areas of their fluorescence (FLD) and light-scattering (LS) fractograms, assuming comparable and optimal UF recovery. Protein- and LDL-associated peaks were evaluated from FLD signals, whereas the EV-related peak was quantified from LS fractograms. To account for the different plasma volumes processed (60 μL for HF5 and 500 μL for SEC), the areas of HF5 fractions were multiplied by a correction factor of 8.3. Additionally, to compensate for the different injection volumes of the ultrafiltered samples (25 μL for HF5 and 20 μL for SEC), the peak areas of SEC fractions were multiplied by 1.25.

2.4. SEC for the separation of EVs from plasma

The SEC was performed according to the manufacturer's instructions (iZON Science, Oxford, UK) and as previously described [33]. In summary, the column (qEVoriginal/70 nm Gen 2 column, Izon) was equilibrated with PBS before loading the 500 μl of processed plasma sample onto the top of the column. Following the manufacturer's instructions, 1.6 ml of fractions containing EVs were collected as indicated (1 × PBS used as an eluent). To maximize the yield of EV, the collected fractions were concentrated by ultrafiltration using MWCO 100 kDa Amicon Ultra-2 centrifugal filters (Millipore, Merck, USA). Finally, all samples were added DMSO (1%) and then stored at −80 °C until further use.

2.5. Nanoparticle tracking analysis (NTA)

Particle enumeration and size were assessed using NanoSight technology (NanoSight NS300-Malvern Panalytical Ltd., Royston, United Kingdom) and nanoparticle tracking analysis software (NTA Proprietary Software-Malvern Panalytical Ltd.). Each sample, diluted in 0.1 μm filtered isotonic PBS, was acquired in triplicate for 60 s with a flow rate of 30 (arbitrary unit). Data are presented as mean ± S.D.

2.6. Transmission electron microscopy of the isolated EVs

Transmission electron microscopy (TEM) analysis of the isolated EVs was also performed. The samples were processed by adding one drop of solution (approximately 25 μl) on a 400-mesh hole film grid; after staining with 2% uranyl acetate (for 2 min) the sample was observed with a Tecnai G2 (FEI) transmission electron microscope operating at 120 kV. Images were captured with a Veleta (Olympus Soft Imaging System) digital camera.

2.7. Determination of protein content of the isolated EVs

The protein concentrations of isolated EVs were quantified using BCA™ Protein Assay Kit (Thermo Fisher Scientific Inc., Waltham, MA, USA). The assay was performed according to the manufacturer's instructions. The sample were diluted 1:5 in PBS in a final reaction volume of 200 μl. The colour developed within 30 min at 37 °C. Absorbance was measured at 560 nm using the Glomax Multidirection System (Promega Corporation, Madison, WI, USA).

2.8. Western Blotting of the isolated EVs

Protein lysates were separated by sodium dodecyl sulfate–polyacrylamide gel electrophoresis (NuPAGE™ Bis-Tris Mini Protein Gels, 4–12%, Thermo Fisher Scientific, USA) and transferred to a nitrocellulose membrane. Samples were normalized and 25 μg total protein per

Table 1
Parameters of the HF5 separation method for plasma fractionation.

Steps	Focus (mL/min)	Focus-injection (mL/min)	Elution (mL/min)	Elution (mL/min)	Elution (mL/min)	Elution-injection (mL/min)
Flow rate	Vc = 0.35 Vx = 0.8 Time = 0.5 min	Vc = 0.35 Vx = 0.8 Time = 2.5 min	Vc = 0.35 Vx = 0.55 to 0.05 Time = 8 min	Vc = 0.35 Vx = 0.05 to 0.03 Time = 14 min	Vc = 0.35 Vx = 0 Time = 6 min	Vc = 0.35 Vx = 0 Time = 2 min

lane was loaded for Western blot analysis. The following antibodies were used: CD9 (1:1000, Cell Signalling Technology, Danvers, MA, USA), TSG101 (1:1000, BD Bioscience, San Jose, CA, USA), ALIX (1:1000, Cell Signalling Technology, Danvers, MA, USA) and ApoA-1 (1:1000, Santa Cruz Biotechnology). Following goat anti-rabbit and goat anti-mouse HRP conjugated secondary antibodies (System Biosciences) were used at 1:10.000 dilution. SuperSignalTM West Femto Maximum Sensitivity Substrate kit (Thermo Fisher Scientific, USA) was used for detection by a ChemiDoc Imaging System (Bio-Rad, USA).

2.9. Multiplex surface marker analysis of the isolated EVs

Plasma-isolated EVs were analyzed using the human MACSPlex Exosome Kit (Miltenyi Biotec, Bergisch-Gladbach, Germany) according to the manufacturer's instructions and as previously described [33]. This bead-based assay enables the simultaneous detection of 37 surface markers: CD1c, CD2, CD3, CD4, CD8, CD9, CD11c, CD14, CD19, CD20, CD24, CD25, CD29, CD31, CD40, CD41b, CD42a, CD44, CD45, CD49e, CD56, CD62p, CD63, CD69, CD81, CD86, CD105, CD133.1, CD142, CD146, CD209, CD326, HLA-ABC, HLA-DR DP DQ, MCSP, ROR1 and SSEA-4). Samples were normalized, and 4 μg of total protein per sample were used for protein surface profiling. This method provides a detailed and standardized approach to the quantitative and qualitative analysis of EVs, utilizing advanced flow cytometry to assess multiple surface proteins simultaneously.

2.10. Cell culture

The mouse RAW 264.7 macrophage cell line was obtained from the American Type Culture Collection (ATCC, USA #TIB 71). Cells were cultured in MEM α (Minimum Essential Medium α) supplemented with 10% fetal bovine serum (FBS). and plated in T25 flask at a density of 2 x 10^5/ml. The culture was maintained at 37 °C in an incubator with a humidity level and CO2 concentration of 5%.

2.11. EV uptake in RAW 264.7 cells

EVs were labeled using the PKH67 Green Fluorescent Cell Linker Midi Kit (Sigma-Aldrich). EVs were resuspended in 100 μL Diluent C. PKH67 dye was prepared at a final concentration of 2 μM in Diluent C and mixed with the EV suspension (≈10^7 total EVs). After 5 min at room temperature, the reaction was stopped by adding 500 μL of 5% BSA in PBS. Labeled EVs were washed twice with PBS and concentrated using 30 kDa MWCO ultrafiltration. RAW 264.7 cells were then incubated with PKH67-labeled EVs in serum-free medium for 24 h at 37 °C. Following incubation, cells were collected and analyzed for uptake percentage by flow cytometry (FITC channel), according to standard procedures. As a negative control, PBS was processed and stained with PKH67 using the identical labeling, quenching, washing, and concentration steps and applied to cells in parallel.

2.12. Nitric Oxide production assay

RAW 264.7 cell lines were plated in a 96-well plate with a density of 4×10^4 cells per well and incubated overnight. In following, cells were treated with optimum concentration of 1×10^9 and 3×10^9 particles/ml of EVs for 24 h in the presence or the absence of 100 ng/mL lipopolysaccharides (LPS). The supernatant was then used for the detection of Nitric Oxide (NO) using Griess assay reagents (Promega Corporation, Madison, WI, USA). Briefly, the supernatants in each group were collected and mixed with the same volume of Griess reagent. The nitrite concentration was measured at an absorbance of 560 nm using Glomax Multidirection System (Promega Corporation, Madison, WI, USA).

2.13. Statistics

Data were analyzed with Prism GraphPad 10.2.0 Windows (GraphPad Software, Inc., La Jolla, CA, USA). Due to the small sample size, the data were analyzed using the non-parametric Mann-Whitney test where two groups were compared. *P*-values ≤ 0.05 were considered statistically significant and are indicated on the graphs as reported by the analysis software: *p < 0.05, **p < 0.01, ***p < 0.001, ****p < 0.0001.

3. Results

3.1. General and clinical characteristics of study subjects

General and laboratory data from PV patients at diagnosis (n = 10) and HDs (n = 6) are reported in Table S1. Complete blood count analysis revealed a significant increase in white blood cell count, red blood cell count, hemoglobin, hematocrit, and platelet count in PV patients compared to HDs.

3.2. HF5 approach for plasma fractionation and selective isolation of particles

Plasma samples from both PV patients (n = 10) and HDs (n = 6) were injected into the HF5 platform, as above described. The separative profile of plasma at 280 nm (Fig. 1A) exhibits two primary peaks at 4 and 11.8 min, with no significant differences observed between the two sample types. The first peak is mainly composed of albumins and immunoglobulins, as confirmed by injecting an HSA and IgG mixture prepared at the same average protein concentration as plasma and analyzed under identical conditions (data not shown).

Since FFF theory can correlate the hydrodynamic radius with the retention time, it was possible to calibrate the separative method (Fig. 1B) to understand the retention time of the analytes. From this correspondence, the second peak was attributed to species with a diameter comprised between 30 and 100 nm, dimension coherent with that of EVs [34] but also lipoproteins [35] and big immunoglobulins like IgM [36]. Considering the characteristics of this isolation method, the 11–17 min collection window was selected to optimize the process and ensure accurate and reliable fraction acquisition. Flow cytometry analysis of CD9, CD63, and CD81 expression at different time points—before 11 min, between 11 and 17 min, and after 17 min—revealed that the 11–17 min window exhibited the highest expression levels, further validating its selection (Data not shown). The gyration radius associated with the collected fractions displays material with an average diameter of ~50 nm confirming the previous attribution (Fig. 1B). The 3D spectrum (Fig. 1C) outlines the chemical composition of the two bands, with both exhibiting an absorption maximum at 280 nm, a characteristic signal of proteins.

These results demonstrate that the HF5 method can be successfully used for targeted isolation of particles from small amount of human plasma.

3.3. Size, enumeration, morphology and cell uptaking of HF5- and SEC-isolated EVs

We then characterized the particles isolated from plasma using HF5 or SEC. Marker expression and morphology were assessed according to the latest Minimum Information for Studies of Extracellular Vesicles' (MISEV) guidelines [37].

We first evaluated the concentration and size of the particles isolated from the plasma of PV patients and HDs using the HF5 method. The results show no significant differences between the patient and control samples (Fig. 2A and B). Western Blot (Fig. 2C) analysis of the EV surface marker, CD9, and EV internal markers TSG 101 (protein of tumor susceptibility gene 101) and ALIX (ALG-2 interacting protein X) demonstrated the presence of *S*-EVs. Co-isolation of the expression of

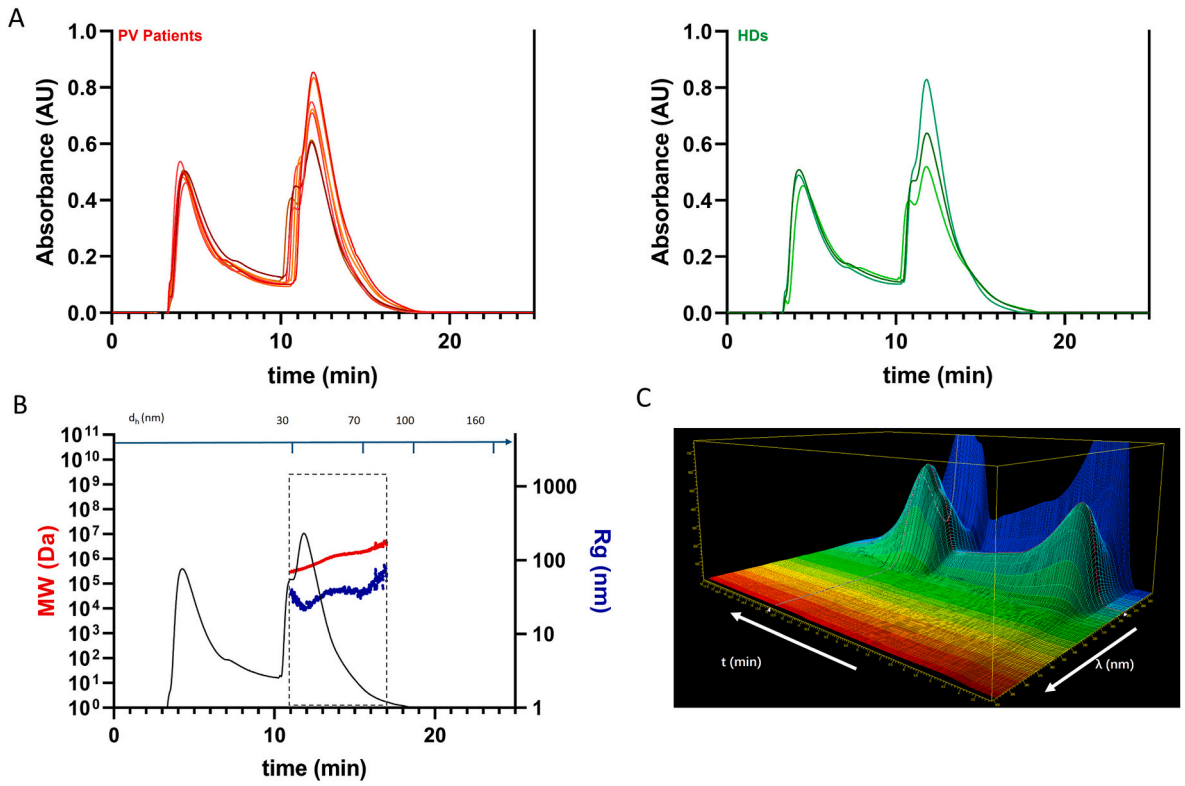

Fig. 1. *Patient and HD plasma fractionation by HF5.* (**A**) UV fractograms obtained from the HF5 analysis of plasma, in green for HDs (n = 3) and in red for PV (n = 7) patients (each line is obtained from the analysis of one Patient or HD plasma sample); (**B**) Separative method size calibration (dh stands for hydrodynamic diameter) and fraction collection window (dashed square) overlapped on a representative HD's plasma UV fractogram (black solid line). The blue and red dotted profiles display respectively the gyration radius (Rg) and molecular weight (MW) calculated for the collected fractions; (**C**) Representative 3D spectrum of an HD's plasma sample analyzed with the HF5-multidetection platform. The 3D plot x-axis corresponds to time (t) in minutes and wavelength (λ) in nanometres, while the y-axis corresponds to the absorbance intensity. This spectrum outlines the composition of the two separated bands of plasma, both of which exhibit absorption maxima at 280 nm, a characteristic signal of proteins. (For interpretation of the references to colour in this figure legend, the reader is referred to the Web version of this article.)

apolipoprotein A-I (APOA1) has also been detected. Finally, TEM (Fig. 2D) showed the presence of spherical and cup-shaped morphologies, with sizes ranging from 30 to 100 nm.

Referring to SEC-EVs, once again no significant differences were observed between PV patients and HDs when particle size or concentration were measured (Fig. 3A and B). Western Blot analysis confirmed the expression of small EVs' protein markers (CD9, ALIX, TSG101) in EVs from PV patients and HDs (Fig. 3C). The TEM image shows round cup-shaped EVs (Fig. 3D).

We then analyzed the EV uptake of HF-5 and SEC-EVs by Raw264.7 macrophages using flow cytometry. Figs. 2E and 3E show that the uptake of the PKH67-labeled HF5 EVs from a PV patient is comparable to and even superior to the SEC counterpart, confirming the fact that the HF5 vesicles are functionally preserved. These findings confirm that the particles isolated from the plasma of PV patients and HDs using HF5 are EVs and that HF5-derived EVs exhibit general characteristics comparable to those obtained via SEC.

3.4. Chemical characterization of EVs isolated with HF5 and SEC

To physically and chemically characterize the composition of the SEC- and HF5-derived fractions from both PV patients (n = 7) and HDs (n = 3), the HF5-multidetection system was used. Focusing HF5-isolated EVs, UV fractograms at 280 nm of the HF5-derived fractions were characterized by the presence of three peaks eluting at 8, 10 and 12 min (Fig. 4A, green line). No significant differences between PV and HD samples in the UV fractograms (Fig. S1A). The 3D spectrum (Fig. 4C) revealed the presence of proteins in peaks 1, 2 and 3. The first two peaks are mainly associated with HSA and IgG, as they exhibit the same retention time and molecular weight distribution as these two proteins (Fig. S1B). The average mass calculated for the first and second peak of the samples is respectively 50 kDa and 150 kDa, which align with the attribution. Peak 3, on the other hand, is characterized by a strong light scattering (LS) signal (Fig. 4A, black line) and a protein-specific spectrum (Fig. 4C) with a relative maximum at ~ 470 nm (Fig. S2), which is probably due to the β-carotene-binding protein in Low Density Lipoproteins (LDL) [38,39]. The average molecular weight of peak 3 (Fig. 4B, red columns) and the gyration radius (Fig. 4B blue columns) for the patients are, respectively, 1.3 ± 0.4 MDa and 13.5 ± 0.7 nm, while for the HD samples are 1.4 ± 0.2 MDa and 13.6 ± 0.5 nm. This partially confirms the previous attribution considering the presence of coelution between LDL and IgM. The analysis of LS signals (Fig. 4A black line) reveals the presence of material without UV absorption, observed after the third UV peak at 12 min, and identified as peak 4. This signal is characterized by an average gyration radius around 23 ± 2 nm for HDs and 25 ± 4 nm for PV patients (Fig. 4B), testifying the presence of material with a size aligned with that of EVs. Although the UV signal, which provides quantitative information, is very similar between patients and HDs, we noticed that PV samples consistently show a more pronounced peak 4 at light scattering. LS signals are closely related to size information and could indicate a more consistent vesicular population in patients' samples.

For LS signals, another peak was found around 26 min, called peak 5 (Fig. 4A). This is related to the field release step of the HF5 separation method, and is due to fully retained species, which can elute only when Vx = 0. This peak intensity, both in UV and LS, in this case, should be as low as possible because it is related to high MW/high radius material, which is a sign of sample aggregation. In terms of method

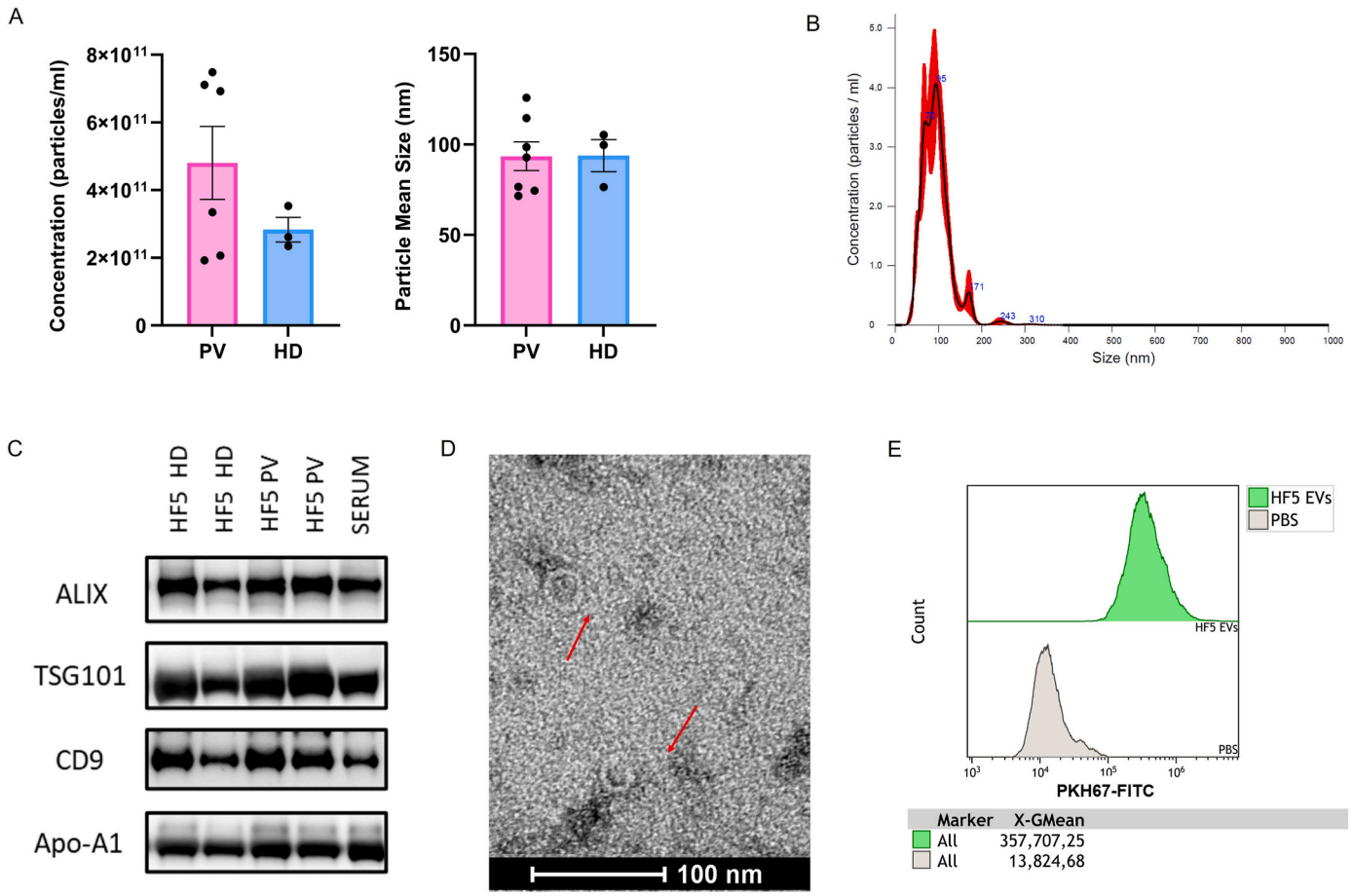

Fig. 2. *Characterization of EVs isolated from the plasma of PV patients and HDs by HF5 method.* (**A**) Size distribution (nm) and particle concentration (particles/ml) of particles from PV ($n = 6$) and HDs ($n = 3$) samples are given; (**B**) Representative NTA histogram reporting size and concentration of particles isolated from the plasma of a PV patient; (**C**) Western Blot revealed that the isolated EVs are enriched in TSG101, ALIX and CD9 EV markers. APO-A1 signal was also present. Serum from one HD showed positivity for all markers; (**D**) Morphological characterization of the isolated PV EVs through TEM (scale bar 100 nm). Arrows exemplarily highlights vesicular structures **.(E)** EV uptake by RAW 264.7 cells. Representative flow cytometry analysis (fluorescence intensity [FITC] vs. counts) showing the uptake of PKH67-labeled EVs isolated from a PV patient using HF5. PBS-treated cells served as a negative control.

reproducibility, UV fractograms at 280 nm of SEC-derived (Fig. S3A) fractions showed a lower reproducibility between samples compared to those of HF5.

Focusing on SEC-EVs, the UV profiles at 280 nm are characterized by the presence of four peaks; the first three are present for all the samples, having a retention time respectively of 8, 10, and 12 min, while the fourth is not consistently observed (Fig. 5A green line). As for HF5-derived fractions, the first two peaks are due to HSA and IgG, indeed, both samples elute at the same retention time as the protein mix (Fig. S3B), indicating similar properties, and exhibit the characteristic absorbance typical of these proteins (Fig. 5C).

The third peak presented characteristics like the counterpart peak in HF5-derived fractions. In fact, it has two absorbance maxima at 280 nm and around 470 nm (Fig. S4), and hence it is attributed to LDL. In fact, the average molecular weight (Fig. 5B, red columns) and gyration radius (Fig. 5B, blue columns) calculated for PV patients are respectively 3 ± 1 MDa and 15 ± 4 nm, while for HDs they are 2.1 ± 0.3 MDa and 11 ± 5 nm, which are consistent with the attribution.

Regarding the HF5 fractions, peak 4 in SEC samples is also associated with EVs. It is characterized by an average gyration radius of 33 ± 4 nm for HDs and 31 ± 3 nm for patients with PV (Fig. 5B), The trend observed in the patient and HD LS fractograms of the HF5 fractions is not evident in the SEC counterparts. Peak 5 has been consistently observed in both HF5- and SEC-derived fractions (Figs. 4A–5A). It is very low in HF5, as expected. Focusing on the SEC-derived fractions, we can see an intense band in the LS, likely due to aggregated material that elutes in the field-release step of the FFF method.

When comparing SEC- and HF5-derived fractions using integrated peak areas scaled for the different processed plasma volumes, both methods yielded comparable amounts of EVs. However, HF5 fractions exhibited a higher relative protein content, as indicated by the larger areas of Peaks 1 and 2 (Fig. S5), whereas SEC fractions showed a greater proportion of aggregated material, reflected by a more pronounced Peak 5. The analysis of the HF5 EV fraction shows how this population is not completely resolved from HSA and IgG, which are naturally present in large amounts in plasma, since these two proteins are present in the re-injection following ultrafiltration. However, they do not influence the stability, recovery, and size characterization of the EV. This suggests that in studies where both representativeness and preservation of protein structure are essential, HF5 can reveal additional, otherwise hidden, information.

3.5. *Surface protein profiling of HF5- and SEC- isolated EVs*

To further characterize the EVs isolated from patients and HDs using HF5 or SEC, we analyzed their protein surface marker profile using a multiplex beads-based assay.

Focusing on EVs isolated using HF5, the mean fluorescence intensity (MFI) of 20 of the 37 measured markers was higher than the isotype control, indicating their presence in recovered vesicles (data not shown).

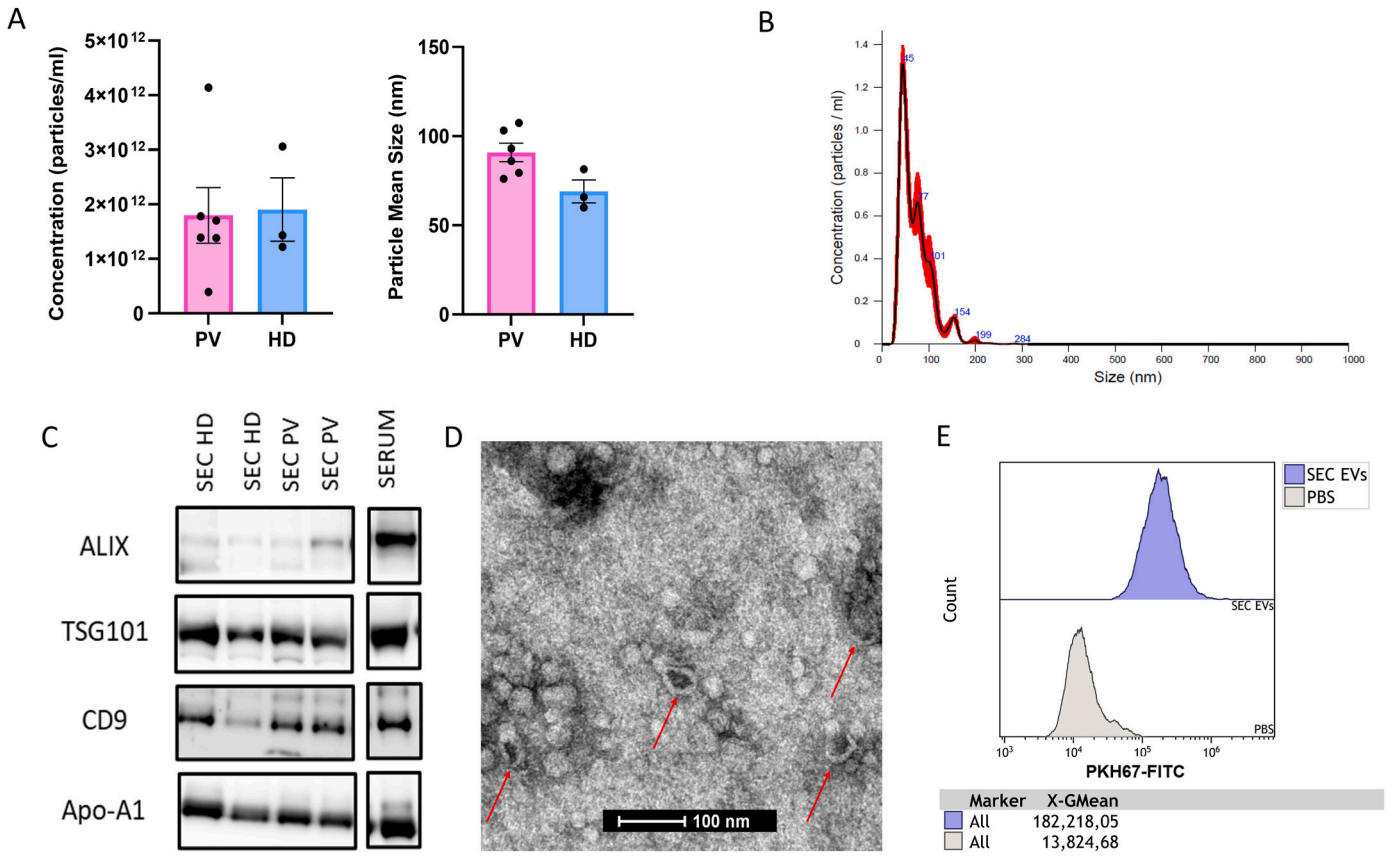

Fig. 3. *Characterization of EVs isolated from the plasma of PV patients and HDs by SEC.* (**A** and **B**) Concentration and size of the particles isolated from the plasma of HDs (N = 3) and PV patients (N = 7); **C**) WB analysis of EV markers in EVs isolated from PV patients and HDs; (**D**) TEM analysis showing round and cup-shaped EVs of a PV patient. **(E)** EV uptake by RAW 264.7 cells. Representative flow cytometry analysis (fluorescence intensity [FITC] vs. counts) showing the uptake of PKH67-labeled EVs isolated from a PV patient using SEC. PBS-treated cells served as a negative control.

Furthermore, as shown in (Fig. 6A and B), these markers were expressed in nearly all tested subjects, reinforcing their robust presence in the data demonstrate that the expression of all platelet markers (CD62P, CD41b, and CD42a) increased in PV EVs in comparison with the HD counterparts; however, only CD42a showed a significant. The expression of the EV marker CD81 was also significantly increased in PV patients ($p < 0.001$).

The phenotypic characterization of the EVs isolated by SEC revealed that the MFI signals for 34 of 37 markers were higher compared to their respective isotype controls, indicating that the EVs isolated by SEC are enriched with most of the evaluated markers (data not shown). As shown in Fig. 7A and B, EV-associated markers and platelet markers were increased in PV EVs compared to HD. However, only the CD63, CD9 and CD42a markers demonstrated a significant increase in PV EVs, while a trend toward significance was observed for CD81, CD62P, and CD41b. Interestingly, the expression of CD69 adhesion-, CD40 immune- and CD31 endothelial-related markers were also significantly higher in PV EVs (Fig. 7C).

In summary, comparing the phenotype of isolated EVs with the two methods, it is possible to highlight that HF5-isolated EVs gave qualitatively similar results but with lower MFI level for platelet markers and tetraspanins. Furthermore, only SEC-EVs showed a significantly stronger MFI signal for selected leukocyte/immune markers (CD69 and CD40) and endothelial markers (CD31) in PV EVs compared to their counterparts in HD EVs.

3.6. *Inflammatory potential of HF5 EVs*

In order to assess the functionality of HF5 EVs in parallel experiments we studied the in vitro ability of HF5 EVs to modulate the NO production by LPS-stimulated macrophgages (Fig. 8). We found that HF5 EVs from PV patients are able to significantly stimulate the NO production by the recipient cells, showing inflammatory potential.

4. Discussion

The isolation and characterization of EVs remains a challenge in both analytical and biotechnological domains. Developing an isolation technique that requires minimal sample volumes facilitates the isolation of nanoscale biological particles like EVs, leveraging their size and fluid dynamics properties, especially in studies involving patient-derived samples, which are often scarce and critically valuable. On the other hand, efficient separation of distinct EV subpopulations is crucial for comprehensive characterization and functional analysis.

Conventional EV isolation methods like ultracentrifugation, SEC, and polymer precipitation suffer from high variability, co-isolation of contaminants (proteins/lipoproteins), poor reproducibility, and high time/sample volume demands, making difficult the selective recovery of EV subpopulations. Crucially, they lack real-time monitoring and cannot preserve the native structure needed for reliable biomarker discovery. In contrast, HF5 offers precise, reproducible separation based on hydrodynamic size. Its design supports low-volume clinical samples and allows real-time monitoring via integrated detectors. This makes HF5 a high-resolution, native, and integrative platform superior to conventional methods. This work is a pilot study providing the first experimental evidence of HF5's feasibility and potential for plasma EV-based biomarker discovery and liquid biopsy in hematological malignancies, laying the foundation for future clinical validation.

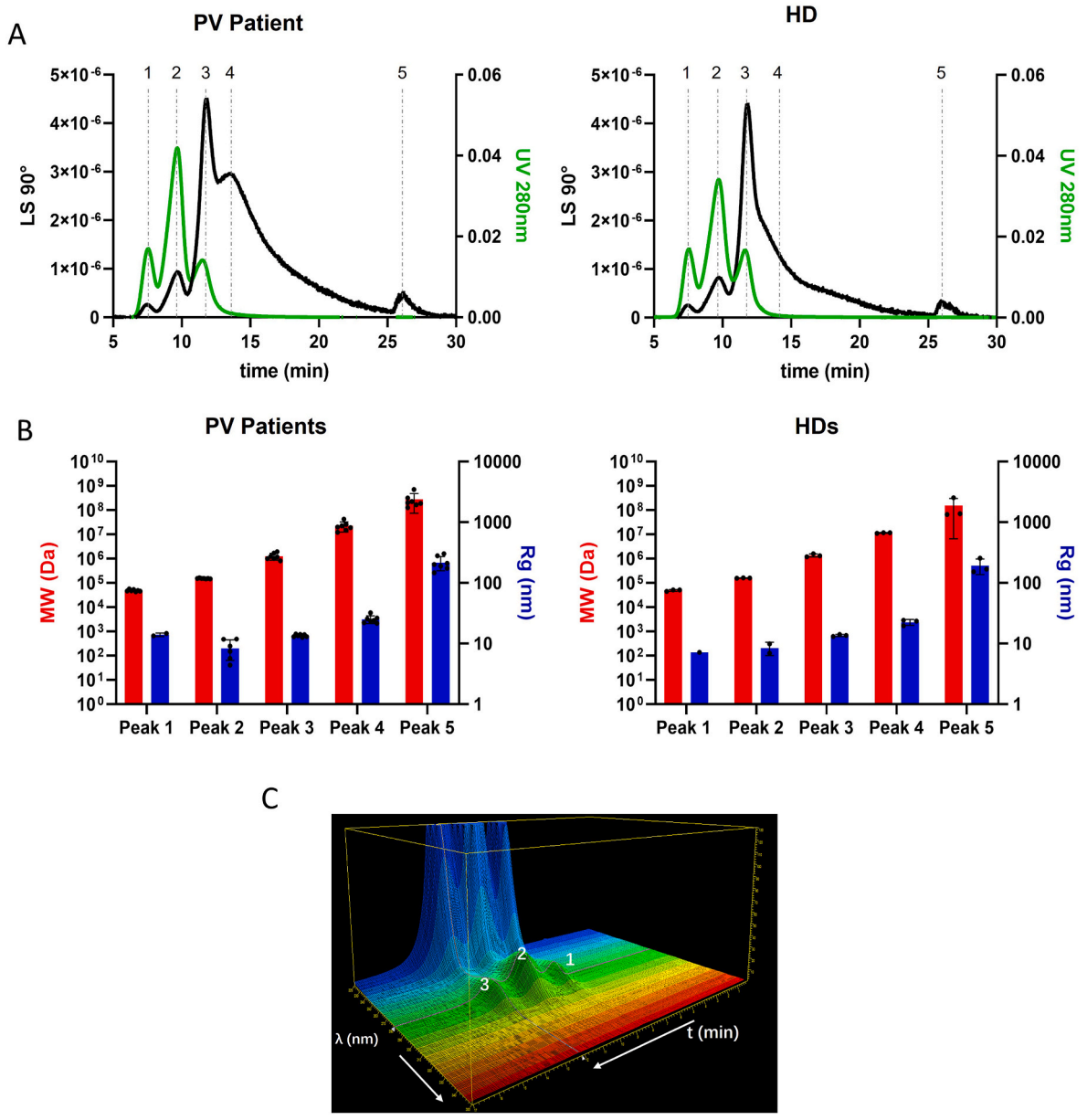

Fig. 4. PV *Patient and HD HF5-derived fraction analysis.* (**A**) Representative UV fractogram at 280 nm (green profile) and Light scattering at 90° (black profile) overlay for one HD and one PV patient of HF5-derived fractions. Each vertical grey dashed line and its associated number correspond to the peaks identified through HF5 analysis; (**B**) Molecular weight (red columns) and gyration radius (blue columns) of the five populations (peaks) from PV Patients (n = 7) and HDs (n = 3); Data presented as mean values ± SEM; (**C**) Representative 3D spectrum of an HD HF5 derived fractions; the numbers correspond to the respective peaks shown in panel A. The spectrum of the x-axis corresponds to time (t) in minutes and wavelength (λ) in nanometres, while the y-axis corresponds to absorbance intensity. Peaks 1, 2 and 3 show maximum absorbance at 280 nm, a characteristic signal of proteins. (For interpretation of the references to colour in this figure legend, the reader is referred to the Web version of this article.)

This study focuses on the efficacy of HF5 as a first line EV isolation method from small amount of plasma from PV patients, highlighting similarities and advantages over conventional SEC. After EV isolation using HF5 or SEC, the selected fraction was characterized for size, concentration, morphology, and expression of tetraspanins. Our data demonstrates that EVs isolated by HF5 and SEC from PV patients and HDs plasma exhibit expected EV properties with similar physicochemical characteristics, while each isolation technique has distinct advantages. Unlike typical isolation techniques, when HF5 was coupled with a UV detector and multiangle light-scattering detectors (UV-MALS), it integrates elements of NTA, providing insights into EV size and composition. The size of HF5- or SEC-derived EVs of PV patients or HDs was always significantly higher using NTA in comparison with HF5. This might be due to the different technologies in evaluating size particles or to the different sensitivity of the method. However, we were unable to detect a significant difference in size between EVs from PV patients or HDs with both techniques. Western blot results revealed that, although SEC is more effective in depleting apolipoproteins than HF5, HF5 samples were more enriched in CD9 and ALIX, small EV markers.

Studying EVs through protein surface profiling using flow cytometry provided significant insights, enabling the analysis of EVs for various cancers, EV-specific, and immune markers. The results of the EV surface protein expression of this study are consistent with previous data reporting that the absolute and relative proportion of platelet-derived EVs are increased in PV patients [28,40–44]. In particular, in our study both SEC- or HF5-isolated EVs showed the same biomarker profile,

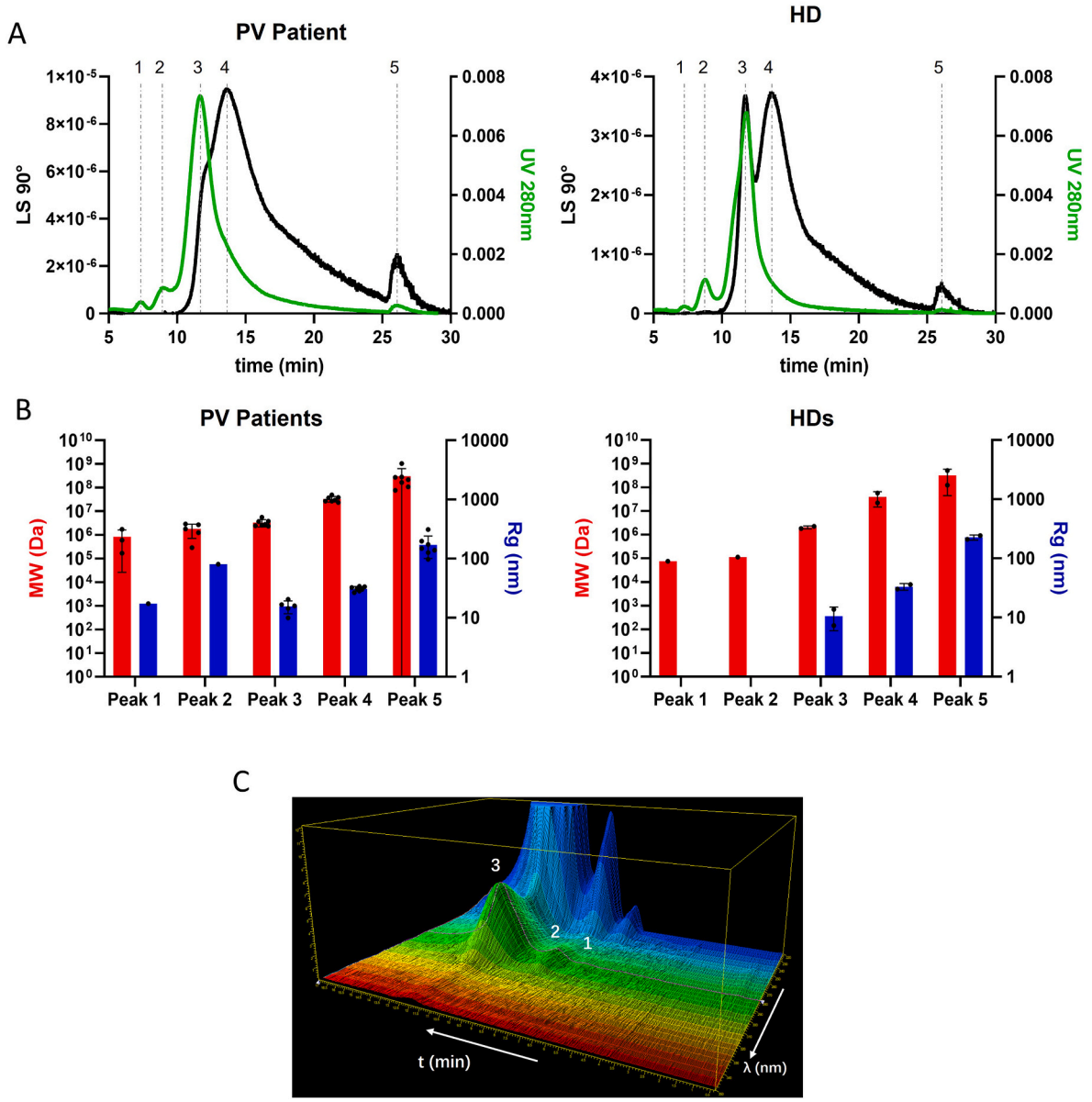

Fig. 5. *PV patient and HD SEC-derived fractions analysis.* (**A**) Representative UV at 280 nm (green profile) and LS at 90° (black profile) fractograms overlay for SEC-derived fractions of one HD and one PV patient. Each vertical grey dashed line and its associated number correspond to the peaks identified through HF5 analysis; (**B**) Molecular weight (red columns) and gyration radius (blue columns) between samples, for PV Patients (n = 7) and HDs (n = 2), of the five found populations. Data presented as mean values ± SEM. Peaks 1 and 2 gyration radii of HDs are not shown since they cannot be calculated from the elaboration software; this is due to very low LS intensity associated with those populations; (**C**) Representative 3D spectrum of an HD SEC-derived fractions; the numbers correspond to the respective peaks shown in panel A. The spectrum of the x-axis corresponds to time (t) in minutes and wavelength (λ) in nanometres, while the y-axis corresponds to absorbance intensity. Peaks 1, 2, and 3 show maximum absorbance at 280 nm, a characteristic signal of proteins. (For interpretation of the references to colour in this figure legend, the reader is referred to the Web version of this article.)

confirming that platelets, and especially activated platelets, play a key role in the microenvironment of the disease. In summary, comparing the phenotype of isolated EVs with the two methods, it is possible to highlight that HF5-isolated EVs gave qualitatively similar results but with lower MFI level for platelet markers and tetraspanins. Furthermore, only SEC-EVs showed a significantly stronger MFI signal for selected leukocyte/immune markers (CD69 and CD40) and endothelial markers (CD31) in PV EVs compared to their counterparts in HD EVs.

Despite the higher total protein (i.e., more co-isolated protein) in the HF5 sample, EV-related markers on the Western blots (e.g., tetraspanins/TSG101/Alix) are stronger, supporting that EV-associated proteins are genuinely enriched and not solely explained by soluble contaminants. For flowcytometry, the overall signal appears weaker in HF5; this is expected because the HF5 condition was 8.3 times lower input volume, so fewer EVs were available for bead capture even though the protein mass per reaction was matched. Importantly, the pattern is consistent: we still detect the PV EV signature related to platelet activation, which aligns with the known higher inflammatory/procoagulant risk in PV patients. Overall, EV-marker bands on WB and the preserved platelet-activation signature in PV, support the biological conclusions and data comparability across assays.

The results obtained support the suitability of HF5 for handling complex biological matrices such as plasma without compromising vesicle integrity or recovery. Despite the theoretical possibility of nonspecific adsorption or shear-related effects associated with flow-based separations, no evidence of such artifacts was observed under

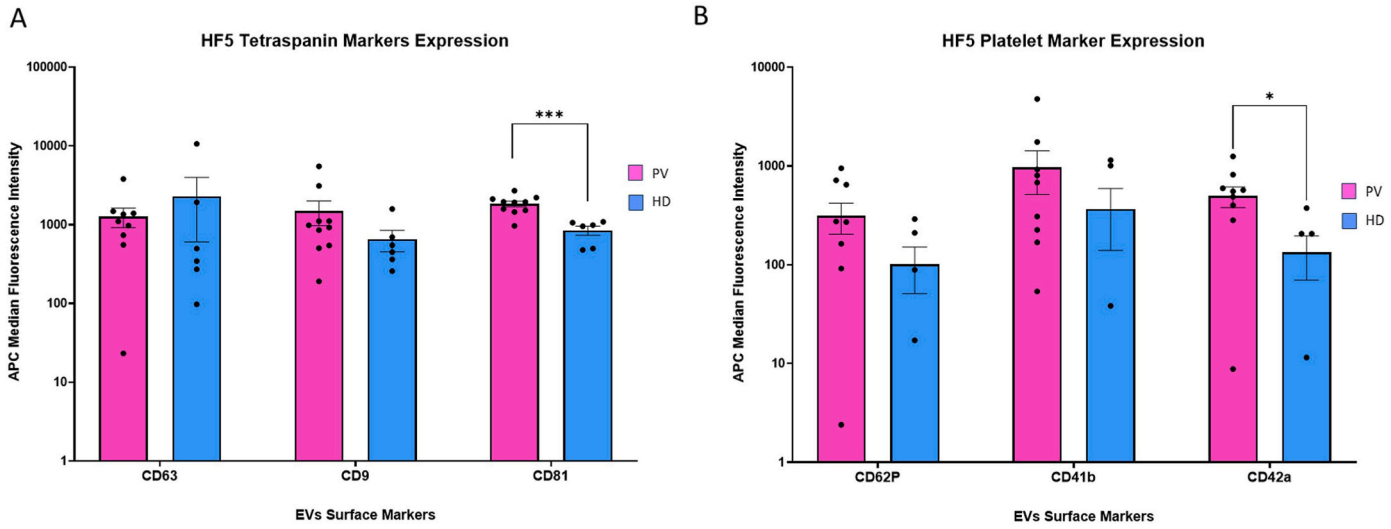

Fig. 6. *Phenotypic analysis of EVs isolated from the plasma of PV patients (n=10) and HDs (n=6) by HF5.* **(A)** Tetraspanin marker expression; **(B)** Platelet marker expression. Reported data are background-corrected median APC fluorescence intensity (MFI) and normalized to respective isotype control. Means (±SEM) *p < 0.05; ***p < 0.001.

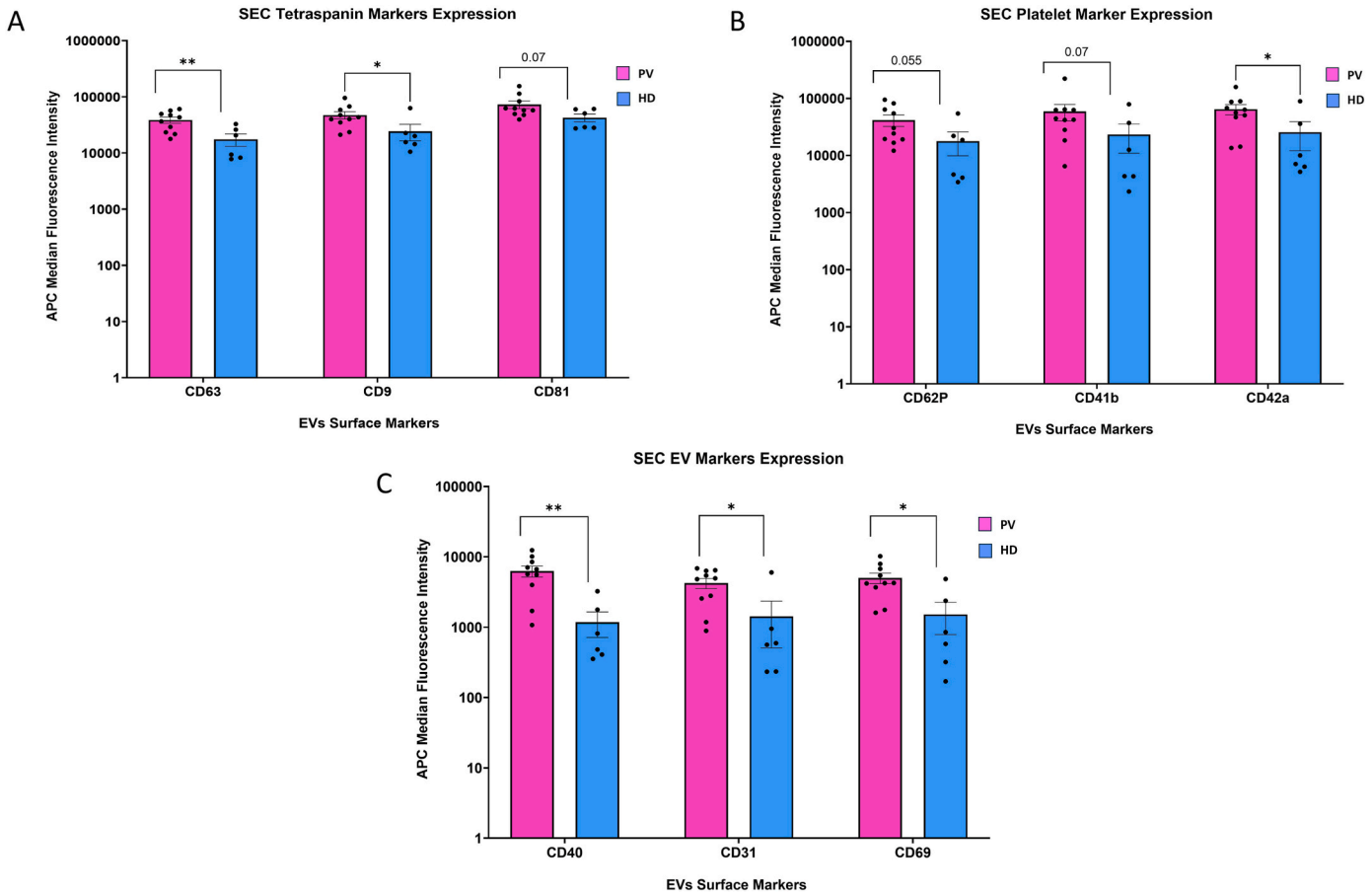

Fig. 7. *Phenotypic analysis of EVs isolated from the plasma of PV patients (n=10) and HDs (n=6) by SEC.* (**A**) Tetraspanin marker expression; (**B**) Platelet marker expression; (**C**) Immune and endothelial marker expression. Reported data are background-corrected median APC fluorescence intensity (MFI) and normalized to respective isotype control. Means (±SEM) *p < 0.05; **p < 0.01; ***p < 0.001.

the applied experimental conditions. The low and fully laminar flow of HF5 ensures gentle fractionation, and the monitoring performed through FIA and FFIA confirmed negligible sample loss or membrane interaction.

Although SEC showed a higher efficiency in removing contaminants such as proteins and lipoproteins, the HF5 method offers the advantage of tunable operational parameters—crossflow rate, focusing time, and channel flow—that can be optimized to obtain EV samples with

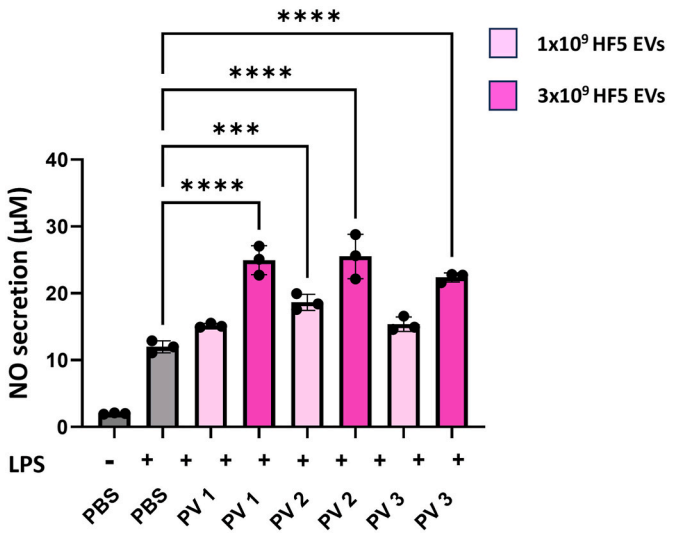

Fig. 8. *Evaluation of NO concentration in resting (-LPS) and stimulated (+LPS) Raw 264.7 macrophages in the presence or the absence of HF-*5 EVs *($1x10^9$ and $3x10^9$) from 3 PV patients.* The NO production was determined using the Griess reagent. The results are expressed as the Mean ± SE. ***$p < 0.001$ and ****$p < 0.0001$ represent significant differences compared with the control group (PBS).

improved purity. This flexibility makes HF5 not only a separation tool but also a versatile analytical platform that can be further implemented or coupled with additional modules to enhance resolution and purity. Indeed, future developments may include the implementation of a Tandem-HF5 configuration, in which two HF5 modules operate sequentially without intermediate ultrafiltration. This setup would enable progressive removal of protein and lipoprotein contaminants and more precise size-based fractionation, while maintaining vesicle integrity and minimizing sample handling. Such an approach could provide highly purified EV preparations suitable for downstream vesicular biomarker analysis or functional studies.

Beyond its use as a gentle EVs isolation method, that we proved offered a solid advantage with respect to SEC, HF5 was also exploited as an analytical platform to assess the impact of conventional isolation procedures, such as SEC, on vesicle integrity and composition. This dual application represents a distinctive feature of the present work, where HF5 served both as a primary isolation tool and as a quasi-tandem quality-control system. HF5 isolation preserved the structure and biomarker distribution of EVs, supporting its role as a reliable and gentle approach for both EV isolation and post-isolation quality assessment.

Interestingly, our functional analysis confirms that HF5-isolated EVs maintain functional integrity compared to their SEC-isolated counterparts, as evidenced by their comparable or superior cellular uptake by Raw264.7 macrophages. Importantly, the functional integrity of these EVs is biologically relevant: we show that PV-derived HF5 EVs possess a significant inflammatory potential, evidenced by their ability to stimulate NO production in LPS-stimulated macrophages, thereby supporting their critical role in the thrombo-inflammatory mechanisms characteristic of PV.

Biologically, this method allowed for fraction-resolved tracing of EVs, which helped preserve their functional landscape and revealed subpopulations carrying a PV-associated platelet signature (CD42a, CD62P, CD41b). Indeed, the study provides new mechanistic insight into PV's microenvironment. Using PV as a clinically relevant testbed, we show that rigorous EV isolation improves fidelity of microenvironmental signals across diseases and helps define promising directions for subsequent research.

5. Conclusions

Here, we demonstrated how HF5 methodology, as first line isolation method, successfully provided intact, characterized and consistent amounts of EVs from a minimal amount of plasma from cancer patients, such as PV patients. Compared to established approaches HF5 excelled in achieving high purity of EV, reduced aggregation of EV, and greater reproducibility. The isolated EVs showed surface protein expression and biological and functional characteristics comparable to those obtained via SEC. Specifically, HF5 enables high-resolution, high-efficiency separation and characterization, which are essential to exploit EVs as diagnostic and therapeutic tools. Moreover, the technique's ability to separate particles based on hydrodynamic size rather than density provides orthogonal and complementary data, which are invaluable for developing new methods for the precise isolation and detailed analysis of EV subpopulations. Notably, HF5 is unique in its ability not only to isolate EVs but also to provide feedback on the consistency of the isolation process across experiments, which ensures reproducibility. Surpassing current protocols, in this pilot study we showed that HF5 is a suitable first line of isolation to be implemented in the clinical setting, where the advantage to both isolate and precisely characterize EVs highlights paves the way for clinical translation and standardized applications.

CRediT authorship contribution statement

Ghazal Narimanfar: Writing – original draft, Visualization, Methodology, Investigation, Formal analysis, Conceptualization. **Anna Placci:** Writing – original draft, Methodology, Investigation, Formal analysis. **Filippo Maltoni:** Writing – review & editing, Investigation, Formal analysis. **Stefano Giordani:** Formal analysis, Conceptualization. **Gianluca Storci:** Investigation. **Barbara Roda:** Writing – review & editing. **Andrea Zattoni:** Writing – review & editing. **Pierluigi Reschiglian:** Writing – review & editing. **Massimiliano Bonafè:** Writing – review & editing. **Francesca Palandri:** Writing – review & editing, Resources, Funding acquisition. **Valentina Marassi:** Writing – original draft, Validation, Supervision, Formal analysis, Conceptualization. **Lucia Catani:** Writing – original draft, Supervision, Resources, Project administration, Investigation, Funding acquisition.

Ethics Approval and consent to Partecipate

The research was approved by the institutional review board of Area Vasta Emilia Centro (AVEC) Ethical Committee (CE AVEC: 1010/2021/Sper/AOUBo) and conducted in accordance with the Declaration of Helsinki. Informed consent was acquired from all subjects involved in the study.

Funding

This work was funded by Emilia-Romagna Region -Bottom Up project (2020), Italy

Declaration of competing interest

The authors declare that they have no known competing financial interests or personal relationships that could have appeared to influence the work reported in this paper.

Acknowledgment

The authors would like to thank AIL Bologna OdV for their valuable support throughout the project.

Appendix A. Supplementary data

Supplementary data to this article can be found online at https://doi.org/10.1016/j.talanta.2025.129004.

Data availability

Data will be made available on request.

References

[1] L. Catani, M. Cavo, F. Palandri, The power of extracellular vesicles in myeloproliferative neoplasms: "crafting" a microenvironment that matters, Cells 10 (9) (2021).
[2] H.C. Hasselbalch, M.E. Bjorn, MPNs as inflammatory diseases: the evidence, consequences, and perspectives, Mediators Inflamm 2015 (2015) 102476.
[3] S. Beck, B. Hochreiter, J.A. Schmid, Extracellular vesicles linking inflammation, cancer and thrombotic risks, Front. Cell Dev. Biol. 10 (2022) 859863.
[4] C. Thery, K.W. Witwer, E. Aikawa, M.J. Alcaraz, J.D. Anderson, R. Andriantsitohaina, et al., Minimal information for studies of extracellular vesicles 2018 (MISEV2018): a position statement of the international society for extracellular vesicles and update of the MISEV2014 guidelines, J. Extracell. Vesicles 7 (1) (2018) 1535750.
[5] Y. Zhang, Y. Liu, H. Liu, W.H. Tang, Exosomes: biogenesis, biologic function and clinical potential, Cell Biosci. 9 (2019) 19.
[6] C. Tricarico, J. Clancy, C. D'Souza-Schorey, Biology and biogenesis of shed microvesicles, Small GTPases 8 (4) (2017) 220–232.
[7] R. Kalluri, K.M. McAndrews, The role of extracellular vesicles in cancer, Cell 186 (8) (2023) 1610–1626.
[8] A. Alberro, L. Iparraguirre, A. Fernandes, D. Otaegui, Extracellular vesicles in blood: sources, effects, and applications, Int. J. Mol. Sci. 22 (15) (2021).
[9] M. Holcar, M. Kanduser, M. Lenassi, Blood nanoparticles - influence on extracellular vesicle isolation and characterization, Front. Pharmacol. 12 (2021) 773844.
[10] T. Tzaridis, D. Bachurski, S. Liu, K. Surmann, F. Babatz, M. Gesell Salazar, et al., Extracellular vesicle separation techniques impact results from human blood samples: considerations for diagnostic applications, Int. J. Mol. Sci. 22 (17) (2021).
[11] V. Marassi, S. Maggio, M. Battistelli, V. Stocchi, A. Zattoni, P. Reschiglian, et al., An ultracentrifugation - hollow-fiber flow field-flow fractionation orthogonal approach for the purification and mapping of extracellular vesicle subtypes, J. Chromatogr. A 1638 (2021) 461861.
[12] J. Fukuda, T. Iwura, S. Yanagihara, K. Kano, Separation and quantification of monoclonal-antibody aggregates by hollow-fiber-flow field-flow fractionation, Anal. Bioanal. Chem. 406 (25) (2014) 6257–6264.
[13] E. Oeyen, K. Van Mol, G. Baggerman, H. Willems, K. Boonen, C. Rolfo, et al., Ultrafiltration and size exclusion chromatography combined with asymmetrical-flow field-flow fractionation for the isolation and characterisation of extracellular vesicles from urine, J. Extracell. Vesicles 7 (1) (2018) 1490143.
[14] A.M. Striegel, On-line coupling of hollow-fiber flow field-flow fractionation and depolarized multi-angle static light scattering (HF5/D-MALS). Proof of principle, J. Chromatogr. A 1730 (2024) 465115.
[15] H. Zhang, D. Lyden, Asymmetric-flow field-flow fractionation technology for exomere and small extracellular vesicle separation and characterization, Nat. Protoc. 14 (4) (2019) 1027–1053.
[16] J. Bian, N. Gobalasingham, A. Purchel, J. Lin, The power of field-flow fractionation in characterization of nanoparticles in drug delivery, Molecules 28 (10) (2023).
[17] S.K. Wiedmer, M.L. Riekkola, Field-flow fractionation - an excellent tool for fractionation, isolation And/Or purification of biomacromolecules, J. Chromatogr. A 1712 (2023) 464492.
[18] V. Marassi, S. Giordani, P. Reschiglian, B. Roda, A. Zattoni, Tracking heme-protein interactions in healthy and pathological human serum in native conditions by miniaturized FFF-Multidetection, Applied Sciences 12 (13) (2022) 6762.
[19] V. Marassi, M. Macis, S. Giordani, L. Ferrazzano, A. Tolomelli, B. Roda, et al., Application of Af4-multidetection to liraglutide in its formulation: preserving and representing native aggregation, Molecules 27 (17) (2022) 5485.
[20] A. Quintas-Cardama, S. Verstovsek, Molecular pathways: jak/stat pathway: mutations, inhibitors, and resistance, Clin. Cancer Res. 19 (8) (2013) 1933–1940.
[21] R. Marchioli, G. Finazzi, R. Landolfi, J. Kutti, H. Gisslinger, C. Patrono, et al., Vascular and neoplastic risk in a large cohort of patients with polycythemia vera, J. Clin. Oncol. 23 (10) (2005) 2224–2232.
[22] H. Geyer, R. Scherber, H. Kosiorek, A.C. Dueck, J.J. Kiladjian, Z. Xiao, et al., Symptomatic profiles of patients with polycythemia vera: implications of inadequately controlled disease, J. Clin. Oncol. 34 (2) (2016) 151–159.
[23] A.M. Vannucchi, From leeches to personalized medicine: evolving concepts in the management of polycythemia vera, Haematologica 102 (1) (2017) 18–29.
[24] F. Palandri, E. Rossi, G. Auteri, M. Breccia, S. Paglia, G. Benevolo, et al., Predictors of response to hydroxyurea and switch to ruxolitinib in HU-Resistant polycythaemia VERA patients: a real-world PV-NET study, Cancers (Basel) 15 (14) (2023).
[25] H.C. Hasselbalch, Perspectives on chronic inflammation in essential thrombocythemia, polycythemia vera, and myelofibrosis: is chronic inflammation a trigger and driver of clonal evolution and development of accelerated atherosclerosis and second cancer? Blood 119 (14) (2012) 3219–3225.
[26] R. Vaidya, N. Gangat, T. Jimma, C.M. Finke, T.L. Lasho, A. Pardanani, et al., Plasma cytokines in polycythemia vera: phenotypic correlates, prognostic relevance, and comparison with myelofibrosis, Am. J. Hematol. 87 (11) (2012) 1003–1005.
[27] E. Pourcelot, C. Trocme, J. Mondet, S. Bailly, B. Toussaint, P. Mossuz, Cytokine profiles in polycythemia vera and essential thrombocythemia patients: clinical implications, Exp. Hematol. 42 (5) (2014) 360–368.
[28] M. Ahadon, S. Abdul Aziz, C.L. Wong, C.F. Leong, Plasma-derived microparticles in polycythaemia vera, Malays. J. Pathol. 40 (1) (2018) 41–48.
[29] Z. Litwinska, K. Luczkowska, B. Machalinski, Extracellular vesicles in hematological malignancies, Leuk. Lymphoma 60 (1) (2019) 29–36.
[30] D. Van Morckhoven, N. Dubois, D. Bron, N. Meuleman, L. Lagneaux, B. Stamatopoulos, Extracellular vesicles in hematological malignancies: EV-Dence for reshaping the tumoral microenvironment, Front. Immunol. 14 (2023) 1265969.
[31] A. Fel, A.E. Lewandowska, P.E. Petrides, J.R. Wisniewski, Comparison of proteome composition of serum enriched in extracellular vesicles isolated from polycythemia vera patients and healthy controls, Proteomes 7 (2) (2019).
[32] S. Giordani, N. Kassouf, A. Zappi, A. Zattoni, B. Roda, D. Melucci, et al., Rapid and green discrimination of bovine milk according to fat content, thermal treatment, brand and manufacturer via colloidal fingerprinting, Food Chem. 440 (2024) 138206.
[33] D. Forte, R.M. Pellegrino, S. Trabanelli, T. Tonetti, F. Ricci, M. Cenerenti, et al., Circulating extracellular particles from severe COVID-19 patients show altered profiling and innate lymphoid cell-modulating ability, Front. Immunol. 14 (2023) 1085610.
[34] L.M. Doyle, M.Z. Wang, Overview of extracellular vesicles, their origin, composition, purpose, and methods for exosome isolation and analysis, Cells 8 (7) (2019).
[35] K.R. Feingold, in: K.R. Feingold, B. Anawalt, M.R. Blackman, A. Boyce, G. Chrousos, E. Corpas, et al. (Eds.), Introduction to Lipids and Lipoproteins, Endotext, South Dartmouth (MA, 2000.
[36] D.M. Czajkowsky, Z. Shao, The human IgM pentamer is a mushroom-shaped molecule with a flexural bias, Proc. Natl. Acad. Sci. U. S. A. 106 (35) (2009) 14960–14965.
[37] J.A. Welsh, D.C.I. Goberdhan, L. O'Driscoll, E.I. Buzas, C. Blenkiron, B. Bussolati, et al., Minimal information for studies of extracellular vesicles (MISEV2023): from basic to advanced approaches, J. Extracell. Vesicles 13 (2) (2024) e12404.
[38] L.B. Sicchieri, A.M. Monteiro, R.E. Samad, A.S. Ito, A.M. Neto, N.D. Vieira Jr., et al., Study of tryptophan lifetime fluorescence following low-density lipoprotein modification, Appl. Spectrosc. 67 (4) (2013) 379–384.
[39] Z. Lotfollahi, APdQ. Mello, E.S. Costa, C.L. Oliveira, N.R. Damasceno, M.C. Izar, et al., Green-banana biomass consumption by diabetic patients improves plasma low-density lipoprotein particle functionality, Sci. Rep. 10 (1) (2020) 12269.
[40] T. Villmow, B. Kemkes-Matthes, A.C. Matzdorff, Markers of platelet activation and platelet-leukocyte interaction in patients with myeloproliferative syndromes, Thromb. Res. 108 (2–3) (2002) 139–145.
[41] M.H. Aswad, J. Kissova, L. Rihova, J. Zavrelova, P. Ovesna, M. Penka, High level of circulating microparticles in patients with BCR/ABL negative myeloproliferative neoplasm - a pilot study, Klin. Onkol. 32 (2) (2019) 109–116.
[42] W. Zhang, J. Qi, S. Zhao, W. Shen, L. Dai, W. Han, et al., Clinical significance of circulating microparticles in Ph(-) myeloproliferative neoplasms, Oncol. Lett. 14 (2) (2017) 2531–2536.
[43] X. Tan, J. Shi, Y. Fu, C. Gao, X. Yang, J. Li, et al., Role of erythrocytes and platelets in the hypercoagulable status in polycythemia vera through phosphatidylserine exposure and microparticle generation, Thromb Haemost 109 (6) (2013) 1025–1032.
[44] J. Kissova, P. Ovesna, A. Bulikova, J. Zavrelova, M. Penka, Increasing procoagulant activity of circulating microparticles in patients with Philadelphia-negative myeloproliferative neoplasms: a single-centre experience, Blood Coagul. Fibrinolysis 26 (4) (2015) 448–453.